Distributing inefficiencies compensation in a grid-tied microgrid: a system of constant references approach

Santiago Benavides, Nicolas Muñoz, Juan Bernardo, León Serna and Salvador Segui

***Abstract*—This research aims to develop a System of Constant References (SoCR) which looks for unbalance and reactive power distributed compensation in MicroGrid (MR) applications. This study is motivated by the need to enhance quality power in MR, looking for cost decreasing, stability increase and environmental impact decrease. Constant References CR are calculated by applying symmetrical components to unbalanced current, modifying zero sequences in a three-phase systems using a operator to lag $\frac{2\pi}{3}$ the zero sequences and applying dq transformation to positive sequence, dq negative transformation to negative sequence and dq transformation to modified zero sequence. This paper shows a MR simulation in OpenModelica software. The simulated MR is composed of the main grid, three grid-follower DC/AC converters (Energy Gateway, EG) and an unbalanced load varying in time; in this simulation, inefficiencies of load changes in time and the EGs compensate inefficiencies equally, validating correct proposal behavior. The SoCR allows the EGs of the MR to contribute in inefficiencies compensation while the EG exchanges energy to the main grid. This feature allows the MR to consider energetic resource availability and enhance quality power at the same time. The distribution of inefficiencies possibility among EGs is a powerful tool which can avoid to install an active power filter for the MR, enhances energy quality, could be proposed like an standard for commercial EG for MR and increases MR key performance indicator.**

***Index Terms*—MR, Microgrid, Efficiency, multi-functional inverter, Inefficiency distribution, Constant References, CR references.**

I. Introduction

GLOBAL generation and consumption policies have been modified along time due to high pollution level and the energy demand raising in all countries around the world. New policies promote renewable energy development, research and use [1], [2], [3], [4], fostering electrical paradigm change from iron-copper centralized system, which thrived whole XX century [5], to electric distributed generation system coordinated by means of communications systems [6], [7], [8]. This change of paradigm requests research due to renewable resources intermittency, instability produced for intermittency and technologies developments according to the new electric paradigm. In the new no centralized scenario, MRs are described as key component of modern electric systems [9], [10]. MRs are electric system of generation, consumption and energy management in low voltage node connected throughout circuit breaker which must accomplish given features, among this, inefficiencies compensation. MRs inefficiencies compensation could be reached out due to EG flexibility. EGs have been developed for several generation application and energy storage with ancillary service, however, EGs in MRs perform as energy gateway between the main grid and energy resource or energy storage. Furthermore, EGs in MRs have the possibility to work as active power filter to enhance quality power. Due to EGs versatility, a MR could distributes inefficiencies among EGs for enhancing power quality, therefore, the need for a methodology to distribute inefficiencies among EGs in a MR is highlighted.

Unbalances and reactive power inefficiencies are usually compensated by means of shunt active power filter, where the filter supplies demanded inefficiencies by load. Literature reports several kinds of unbalance and reactive power compensation. In [11] an unbalanced and reactive power compensation strategies review is presented, which lists control strategies to compensate inefficiencies. In [11] are mentioned unbalanced and reactive power compensation methods as the natural reference frame in abc (NARF), the $a-\beta$ stationary reference frame (STRF), or the dq synchronous reference frame (SRF) and several control strategies applications like PI control, resonant control, repetitive control and alternative control proposals. In [12] a symmetrical components decomposition is used for unbalance compensating. With MR emergence, the literature shows EG application developments for photo-voltaic [13], [14], wind [15] o battery energy storage [14]. Further [16], [17] shows EGs with ancillary services and with unbalance and reactive power compensation ancillary services, however, respect to inefficiencies, EG philosophy aims is to compensate all MR inefficiencies, which means a bigger power of EG which will be unused when there will not be energy resource. MR reactive power compensation could be done scheduling a percentage of reactive power supplied by each EG, furthermore, in [18] is proposed a master-slave system for distributing unbalance and reactive power between EGs by means conservative power theory. Inefficiencies compensation by means of conservative power theory is made by mean of unbalanced signals and time-varying signals as a reference. In the face of this developments, need for unbalances and reactive power inefficiencies distribution among EG in a MR is highlighted due to that EGs inefficiencies contribution could avoid acquiring an active power filter, enhancing quality power and

Manuscript received April XX, 20XX; revised June XX, 20XX. (Write the date on which you submitted your paper for review.) This work was supported in part by the U.S. Department of Commerce under Grant BS123456 (sponsor and financial support acknowledgment goes here). Paper titles should be written in uppercase and lowercase letters, not all uppercase. Avoid writing long formulas with subscripts in the title; short formulas that identify the elements are fine.

M. Shell is with the Department of Electrical and Computer Engineering, Georgia Institute of Technology, Atlanta, GA, 30332 USA e-mail: (see http://www.michaelshell.org/contact.html).

J. Doe and J. Doe are with Anonymous University.

increasing MR key performance indices.

The paper [12] propose a the methodology to develop a SoCR, however, [12] aims to provide a new control strategy for unbalanced load compensation. Therefore, the contribution of this paper is the development of use of SoCR for distributed inefficiencies compensation of reactive power and unbalance in a MR application. SoCR allows to establish a percentage of inefficiencies compensation in a EG while the EG is exchanging energy with the grid, further, SoCR allows to select what inefficiency compensate. This proposal increase load factor of EG in key performance indicator and decrease natural resources consumption in EG production.

This paper is organized as follow: Materials and methods section presents SoCR development, hardware and simulation instantaneous equation are provided and MR application is presented; results section shows two simulation: first one is used for SoCR validation and performing and second one is used for inefficiencies distribution among MR EGs which validates how SoCR performs well-done in MR application. At last, conclusion section summarized more relevant paper aspects. This document has an appendix with theoretical background for dq transformation and symmetrical components, which the aims to guide the reader in a geometrical approach of each one theory, focused on SoCR development way for MR application in inefficiencies distributed compensation.

II. Development, hardware and simulation implementation and use of SoCR in MR applications

This section has three subsections, 1) SoCR development, 2) Algorithms for SoCR implementation in simulation and hardware 3) SoCR in MR application and simulation in OpenModelica.

In this proposal symmetrical components and dq transformation is used for SoCR development. This paper works with fundamental values of currents and considers balanced voltage without harmonics.

From now on, I_A, I_B and I_C are interest fundamental currents of phase A, B y C respectively. I_{1_A}, I_{1_B} and I_{1_C} are positive sequence of fundamental current of phase A, B and C. I_{2_A}, I_{2_B} e I_{2_C} are negative sequences of fundamental current of phases A, B y C. I_{0_A}, I_{0_B} and I_{0_C} are zero sequence of fundamental current of phases A, B y C. At last, a is a phasor operator which unphase $\frac{2\pi}{3}$.

In this paper bold variables are phasors, otherwise, variables are instantaneous values. Subsection "SoCR developments" mixes phasor with instantaneous values in the equations, this to show the proposal sense and development. However, in the subsection "Algorithms for SoCR implementation in hardware and simulation" phasor to instantaneous variable conversion is done, looking for the aim to implement $SoCR$ in hardware or simulation.

Symmetrical components decomposition is done with equations 1, 2, 3 y 4.

$$\begin{bmatrix} \boldsymbol{I_A} \\ \boldsymbol{I_B} \\ \boldsymbol{I_C} \end{bmatrix} = \begin{bmatrix} 1 & 1 & 1 \\ 1 & \boldsymbol{a^2} & \boldsymbol{a} \\ 1 & \boldsymbol{a} & \boldsymbol{a^2} \end{bmatrix} \begin{bmatrix} \boldsymbol{I_{0_A}} \\ \boldsymbol{I_{1_A}} \\ \boldsymbol{I_{2_A}} \end{bmatrix} \tag{1}$$

$$\begin{bmatrix} \boldsymbol{I_{1_A}} \\ \boldsymbol{I_{1_B}} \\ \boldsymbol{I_{1_C}} \end{bmatrix} = \begin{bmatrix} 1 & \boldsymbol{a} & \boldsymbol{a^2} \\ \boldsymbol{a^2} & 1 & \boldsymbol{a} \\ a & \boldsymbol{a^2} & 1 \end{bmatrix} \begin{bmatrix} \boldsymbol{I_A} \\ \boldsymbol{I_B} \\ \boldsymbol{I_C} \end{bmatrix} \tag{2}$$

$$\begin{bmatrix} \boldsymbol{I_{2_A}} \\ \boldsymbol{I_{2_B}} \\ \boldsymbol{I_{2_C}} \end{bmatrix} = \begin{bmatrix} 1 & \boldsymbol{a^2} & \boldsymbol{a} \\ \boldsymbol{a} & 1 & \boldsymbol{a^2} \\ \boldsymbol{a^2} & \boldsymbol{a} & 1 \end{bmatrix} \begin{bmatrix} \boldsymbol{I_A} \\ \boldsymbol{I_B} \\ \boldsymbol{I_C} \end{bmatrix} \tag{3}$$

$$I_{0_A} = I_{0_B} = I_{0_C} = \frac{1}{3}(I_A + I_B + I_C) = I_0 \tag{4}$$

d and q decomposition is made with positive-negative dq transformation shown in equations 5 y 6 respectively [19].

$$T^1_{abc\to dq} = \sqrt{\frac{2}{3}} \begin{bmatrix} \cos(\omega t) & \cos\left(\omega t - \frac{2\pi}{3}\right) & \cos\left(\omega t - \frac{4\pi}{3}\right) \\ -\sin(\omega t) & -\sin\left(\omega t - \frac{2\pi}{3}\right) & -\sin\left(\omega t - \frac{4\pi}{3}\right) \end{bmatrix} \tag{5}$$

$$T^2_{abc\to dq} = \sqrt{\frac{2}{3}} \begin{bmatrix} \cos(\omega t) & \cos\left(\omega t + \frac{2\pi}{3}\right) & \cos\left(\omega t + \frac{4\pi}{3}\right) \\ -\sin(\omega t) & -\sin\left(\omega t + \frac{2\pi}{3}\right) & -\sin\left(\omega t + \frac{4\pi}{3}\right) \end{bmatrix} \tag{6}$$

This proposal comprehension get ease with previous reading of appendix A: geometrical deduction of dq transformation and symmetrical components.

A. SoCR develpment

SoCR is explained by means of figure 1 in three steps. The first step is to decompose unbalanced three-phase current I_A, I_B e I_C in symmetrical components as figure 1, where I_{1_A}, I_{1_B} and I_{1_C} are positive sequence current, I_{2_A}, I_{2_B} e I_{2_C} are negative sequence current, and I_{0_A}, I_{0_B} and I_{0_C} are zero sequence current. The second step is to convert zero sequence current in balanced three-phase system by means of a and a^2. Figure 1 in step two, shows that if I_{0_B} is multiplied by a^2 and I_{0_C} is multplied by a, the zero sequence current is converted to in a balanced three-phase system of positive sequence. The third step consist in to apply dq transformation considering system rotation [19], it means, to apply equation 5 to positive sequence, showed in black in figure 1, and to apply equation 6 for negative sequence, showed in red in figure 1.

Given SoCR procedure, the Constant References CR of SoCR are organized as a vector in equation 7, where I_{1_d} is d component of positive sequence , I_{1_q} is q component of positive sequence, I_{2_d} is d component of negative sequence, I_{2_q} is q component of negative sequence, I_{0m_d} is a d component of modified zero sequence and I_{0m_q} is a q component of modified zero sequence. CR vector will be used for equation formulation and results showing.

$$CR = \begin{bmatrix} I_{1_d} & I_{1_q} & I_{2_d} & I_{2_q} & I_{0m_d} & I_{0m_q} \end{bmatrix} \tag{7}$$

CR calculus is presented in equations 8, 9, 10 and 11 as follow: I_{1_d} and I_{1_q} is presented in equation 8 and I_{2_d} e I_{2_q} is presented in equation 9.

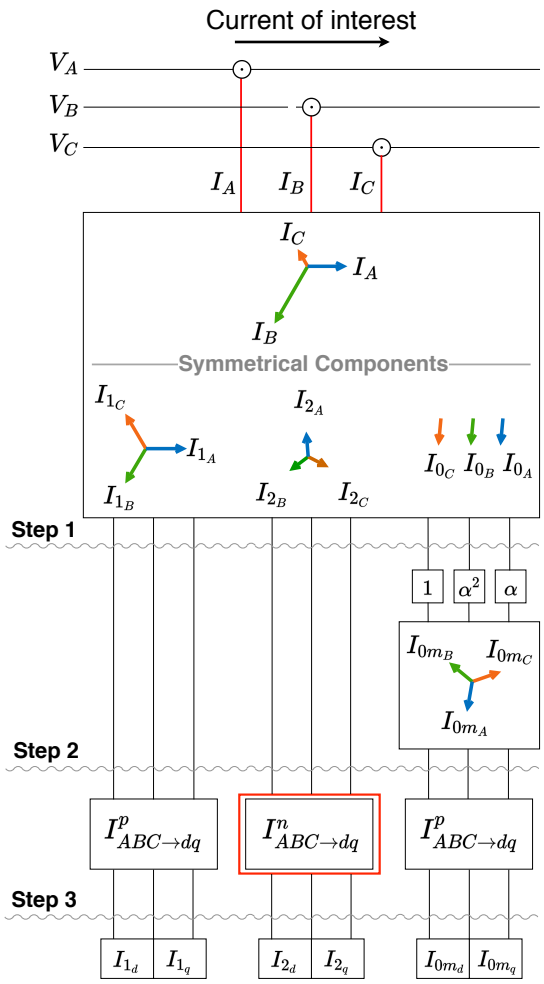

Fig. 1. SoCR proposal. Symmetrical components in step one, zero sequence modification in step two and dq transformation in step three.

$$\begin{bmatrix} I_{1_d} \\ I_{1_q} \end{bmatrix} = T^1_{ABC\to dq} \begin{bmatrix} I_{1_A} \\ I_{1_B} \\ I_{1_C} \end{bmatrix} \tag{8}$$

$$\begin{bmatrix} I_{2_d} \\ I_{2_q} \end{bmatrix} = T^2_{ABC\to dq} \begin{bmatrix} I_{2_A} \\ I_{2_B} \\ I_{2_C} \end{bmatrix} \tag{9}$$

I_{0m_d} and I_{0m_q} calculus requires zero sequence processing as figure 1 suggest. Equation 10 shows a balanced three-phase system calculus from zero sequence components. Equation 10 is a phasorial calculus.

$$\begin{bmatrix} \boldsymbol{I_{0m_A}} \\ \boldsymbol{I_{0m_B}} \\ \boldsymbol{I_{0m_C}} \end{bmatrix} = \begin{bmatrix} 1 & 0 & 0 \\ 0 & \boldsymbol{a^2} & 0 \\ 0 & 0 & \boldsymbol{a} \end{bmatrix} \begin{bmatrix} \boldsymbol{I_{0_A}} \\ \boldsymbol{I_{0_B}} \\ \boldsymbol{I_{0_C}} \end{bmatrix} \tag{10}$$

subsequently, equation 11 shows I_{0m_d} and I_{0m_q} calculus considering instantaneous values.

$$\begin{bmatrix} I_{0m_d} \\ I_{0m_q} \end{bmatrix} = T^1_{ABC\to dq} \begin{bmatrix} I_{0m_A} \\ I_{0m_B} \\ I_{0m_C} \end{bmatrix} \tag{11}$$

In SoCR application, the three-phase current of interest is mapped from ABC domain to CR domain, looking for distributing inefficiencies among EGs. Consequently, after the distribution and assignment of CR to each EG, each EG maps current it must compensate from CR domain to ABC domain to establish the magnitude of instantaneous current it must provide to the main grid.

The current to be supplied by each EG to the power grid is calculated in the reverse way to the figure 1, that is, from step 3 to step 1, as follows: 3) positive inverse transform dq is applied to the components I_{1_d}, I_{q_q} and to the components I_{0m_d} and a negative inverse transform dq is applied to the components, I_{2_d}, I_{2_q}; 2) the modified zero sequence is transformed into zero sequence and 1) the symmetrical components are added to form an unbalanced three-phase current which will be the reference of each EG.

Equation to do inverse of step 3), it means, calculus to obtain the three balanced three-phase systems: currents of positive sequence, currents of negative sequence and currents of modified zero sequences are presented in equations 12, 13 y 14.

$$\begin{bmatrix} I_{1_A} \\ I_{1_B} \\ I_{1_C} \end{bmatrix} = T^{1}_{ABC\to dq}{}^{-1} \begin{bmatrix} I_{1_d} \\ I_{1_q} \end{bmatrix} \tag{12}$$

$$\begin{bmatrix} I_{2_A} \\ I_{2_B} \\ I_{2_C} \end{bmatrix} = T^{2}_{ABC\to dq}{}^{-1} \begin{bmatrix} I_{2_d} \\ I_{2_q} \end{bmatrix} \tag{13}$$

$$\begin{bmatrix} I_{0m_A} \\ I_{0m_B} \\ I_{0m_C} \end{bmatrix} = T^{1}_{ABC\to dq}{}^{-1} \begin{bmatrix} I_{0m_d} \\ I_{0m_q} \end{bmatrix} \tag{14}$$

Inverse of step 2) consist in calculus of current of zero sequence from current of modified zero sequence. this step is shown in equation 15. Is important to highlight that I_{0_A}, I_{0_B} and I_{0_C} are equals.

$$\begin{bmatrix} \boldsymbol{I_{0_A}} \\ \boldsymbol{I_{0_B}} \\ \boldsymbol{I_{0_C}} \end{bmatrix} = \begin{bmatrix} 1 & 0 & 0 \\ 0 & \boldsymbol{a} & 0 \\ 0 & 0 & \boldsymbol{a^2} \end{bmatrix} \begin{bmatrix} \boldsymbol{I_{0m_A}} \\ \boldsymbol{I_{0m_B}} \\ \boldsymbol{I_{0m_C}} \end{bmatrix} \tag{15}$$

At last, inverse of step 1) consist in calculus of currents I_A, I_B e I_C using equation 16. The currents I_A, I_B and I_C are currents that each EG must supply to the main grid.

$$\begin{bmatrix} I_A \\ I_B \\ I_C \end{bmatrix} = \begin{bmatrix} I_{0_A} \\ I_{0_B} \\ I_{0_C} \end{bmatrix} + \begin{bmatrix} I_{1_A} \\ I_{1_B} \\ I_{1_C} \end{bmatrix} + \begin{bmatrix} I_{2_A} \\ I_{2_B} \\ I_{2_C} \end{bmatrix} \tag{16}$$

B. Algorithms for SoCR implementation in simulation and hardware

The document [20] shows how to instantly calculate symmetric components; [20] shows that the operator a can be instantly calculated as in the equation 17, where the term $e^{j\frac{\pi}{2}}$ is the sine signal with phase-lag $\frac{\pi}{2}$. It is important to note that an electrical system handles sinusoidal signals, therefore, a sine signal with phase-lag $\frac{\pi}{2}$ is calculated with its derivative.

$$a = e^{\pm j\frac{2\pi}{3}} = e^{\pm j(\frac{\pi}{2}+\frac{\pi}{6})} = -\frac{1}{2} \pm \frac{\sqrt{3}}{2}e^{j\frac{\pi}{2}} \quad (17)$$

For example, if there is a phasor signal $\boldsymbol{V}$ multiplied by a as $\boldsymbol{V_{mod}} = \boldsymbol{aV}$, then, V_{mod} is calculated as in equation 18 where $V^{\frac{\pi}{2}}$ is a V signal with phase-lag $\frac{\pi}{2}$.

$$V_{mod} = -\frac{1}{2}V + \frac{\sqrt{3}}{2}V^{\frac{\pi}{2}} \quad (18)$$

Given the tools to instantly represent multiplied phasor variables by a o a^2, the following is to present the equations to find instantly the CR

Step 1) of figure 1 consist of symmetrical components calculation, therefore, the instantaneous calculation of positive, negative and zero sequence is performed using equation 17 in 2 and 3. Instantaneous value of positive and negative sequences is performed by means equations 19 y 20 respectively. Instantaneous value of I_0 is performed using equation 4.

$$\begin{bmatrix} I_{1_A} \\ I_{1_B} \\ I_{1_C} \end{bmatrix} = \frac{1}{3}\begin{bmatrix} 1 & -0.5 & -0.5 \\ -0.5 & 1 & -0.5 \\ -0.5 & -0.5 & 1 \end{bmatrix}\begin{bmatrix} I_A \\ I_B \\ I_C \end{bmatrix} - \frac{\sqrt{3}}{6}\begin{bmatrix} 0 & -1 & 1 \\ 1 & 0 & -1 \\ -1 & 1 & 0 \end{bmatrix}\begin{bmatrix} I_A^{\frac{\pi}{2}} \\ I_B^{\frac{\pi}{2}} \\ I_C^{\frac{\pi}{2}} \end{bmatrix} \quad (19)$$

$$\begin{bmatrix} I_{2_A} \\ I_{2_B} \\ I_{2_C} \end{bmatrix} = \frac{1}{3}\begin{bmatrix} 1 & -0.5 & -0.5 \\ -0.5 & 1 & -0.5 \\ -0.5 & -0.5 & 1 \end{bmatrix}\begin{bmatrix} I_A \\ I_B \\ I_C \end{bmatrix} + \frac{\sqrt{3}}{6}\begin{bmatrix} 0 & -1 & 1 \\ 1 & 0 & -1 \\ -1 & 1 & 0 \end{bmatrix}\begin{bmatrix} I_A^{\frac{\pi}{2}} \\ I_B^{\frac{\pi}{2}} \\ I_C^{\frac{\pi}{2}} \end{bmatrix} \quad (20)$$

Step 2) of figure 1 consist of a modifying of zero sequence current I_0 using a operator by means of equation 10. I_{0m_B} and I_{0m_C} is performed with equations 21 and 22.

$$I_{0m_B} = \frac{1}{2}(I_0) - \frac{\sqrt{3}}{2}I_0^{\frac{\pi}{2}} \quad (21)$$

$$I_{0m_C} = \frac{1}{2}(I_0) + \frac{\sqrt{3}}{2}I_0^{\frac{\pi}{2}} \quad (22)$$

Step 3) consist of using dq transformation of equation 5 and 6 as is suggested by equations 8, 9 and 11 using instantaneous values of positive and negative sequences and zero modified sequence.

Inverse process for references calculus of I_A, I_B and I_C currents that must provide each EG is performed in inverse form of figure 1. Inverse step 3) is to apply positive inverse dq transformation to I_{1_d}, I_{1_q}, I_{0m_d} and I_{0m_q} and negative inverse dq transformation to I_{2_d}, I_{2_q}. Inverse step 2) consist in change of current of modified zero sequence I_{0m} in zero sequence I_0. Equation 15 shows $I_{0_A} = I_{0m_A}$, and equation 4 shows that zero sequences are equal, $I_{0_A} = I_{0_B} = I_{0_C}$, therefore, this step could be done taking into account only phase A of modified zero sequence. At last, invers step 1) consist of 16 application. This equation establish instantaneous references that must provided each EG.

C. SoCR in MR application and simulation in OpenModelica

The figure 2 shows the example of an MR consisting of the main grid, the loads of a building, generation with solar photovoltaic resource and wind generation and energy storage in batteries. The power generation and energy storage in batteries uses an EG as an energy interface. The EG, in addition to injecting active power into the grid, has the ability to compensate for inefficiencies, however, setting the benchmark to each EG for distributing inefficiencies is not trivial. This part of the document presents the utility of CR to distribute the inefficiencies among each of the EG of an MR.

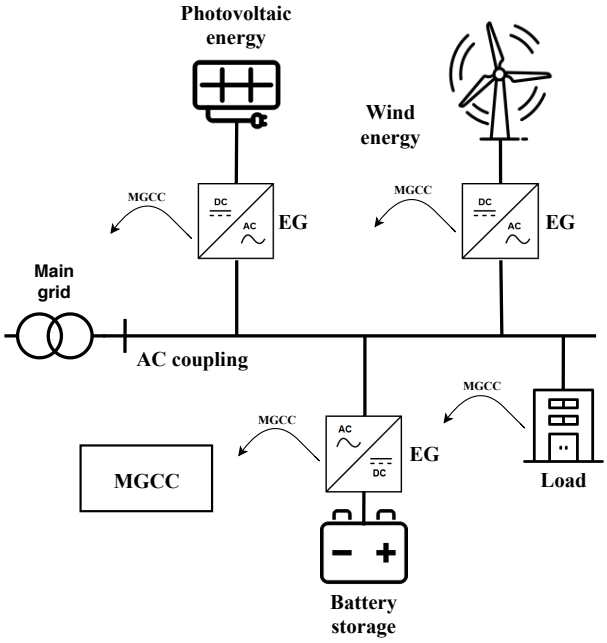

Fig. 2. MG topology with differents generation sources: battery storage, photovoltaic generation and wind generation, Load of the building and a MGCC for MG control.

The CR are applied in the MR of figure 2 as follow: 1) the building load current can be represented by the CR of equation 7. 2) The EG in the figure 2 can deliver or demand active power by means of the CR_1 component and supply the CR_{2-6} inefficiencies demanded by the load; furthermore, it can be established what percentage of inefficiency each EG delivers in any of the CR_{2-6}. Finally, 3) A Microgrid Center Control (MGCC) that evaluates the MG conditions and sets the references of each EG to distribute the inefficiencies and improve the power quality.

In general, a MR with j EG, k loads and a voltage V_{pcc} established by AC coupling bar, seen from CR complies with the equation 23, where ICR^{red} are CR of the main grid current supply, ICR^j are the CR current of each EG and ICR^k are the CR current of the load.

$$ICR_{1-6}^{pcc} = \sum_{i=1}^{j} ICR_{1-6}^{j} + \sum_{i=1}^{k} ICR_{1-6}^{k} \quad (23)$$

Active power of ICR_1^{pcc} can be a positive, negative or zero value, where a positive value means the main grid is providing active power, a negative value means the main grid

is receiving active power and a zero value means there is not energy exchange or MG is self-sufficient. CR consider current flows, therefore, it is important to take into account sensor polarity and EG connection. CR_{2-6} current values are related with inefficiencies, whereby, a MGCC looks for ICR^{grid}_{2-6} be equal to zero; to achieve this objective by means of CR, ICR^{k}_{2-6} values must be distributed among ICR^{j}_{2-6} looking for summation of ICR_{2-6} of load correspond to ICR_{2-6} of EG.

In this document the inefficiencies are distributed in an equitable way to illustrate the proposed method, however, in a real application optimization methods can be used to establish the reference of the EGs looking for that the MG delivers or receives active power maintaining quality power.

The CR are obtained by means of the linear transformations dq and symmetrical components, therefore, the SoCR in this document complies with the superposition property and the equation 23 can be applied for the distributed compensation of inefficiencies.

III. Results

The SoCR is validated in the OpenModelica simulation software with two scenarios: the first scenario simulates the main grid, one load and one EG, with this simulation it is evidenced that the CR are constant values in a stable state and that compensate the inefficiencies; the second scenario simulates the main grid, one variable load and three EGs with solar and wind energy and energy storage in batteries, this simulation shows the use of the SoCR in the distribution of inefficiencies of an RM with a load that varies in time.

To perform the simulations two blocks were built, the blocks are shown in the figure 3. Figure 3 a) shows the reference meter CR; this meter receives three current signals in pins S_a, S_b and S_c from sensors of interest current and delivers the instantaneous value CR; in this block the procedure of figure 1 from step 1 to step 3 is implemented. Figure 3 b) shows an EG that has as input parameters CR; in this block is implemented from step 3 to step 1 of figure 1, in both cases, considering the instantaneous symmetric components equations.

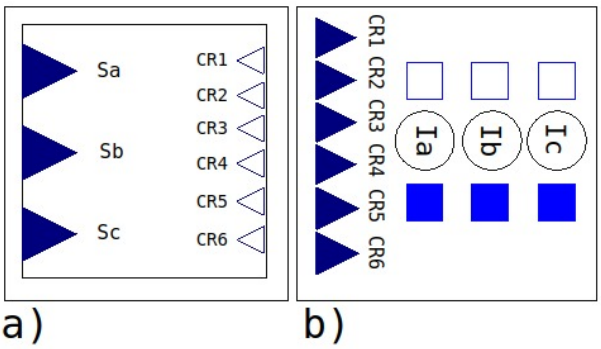

Fig. 3. Builded block created in OpenModelica for SoCR validation. a) meter of CR y b) EG for SoCR, this block receive CR as input.

A. Validation of SoCR using the main grid, one load and one EG

The figure 5 is divided into four blocks: 1) Electrical Grid, 2) EG, 3) a MGCC that distributes CR among the MR

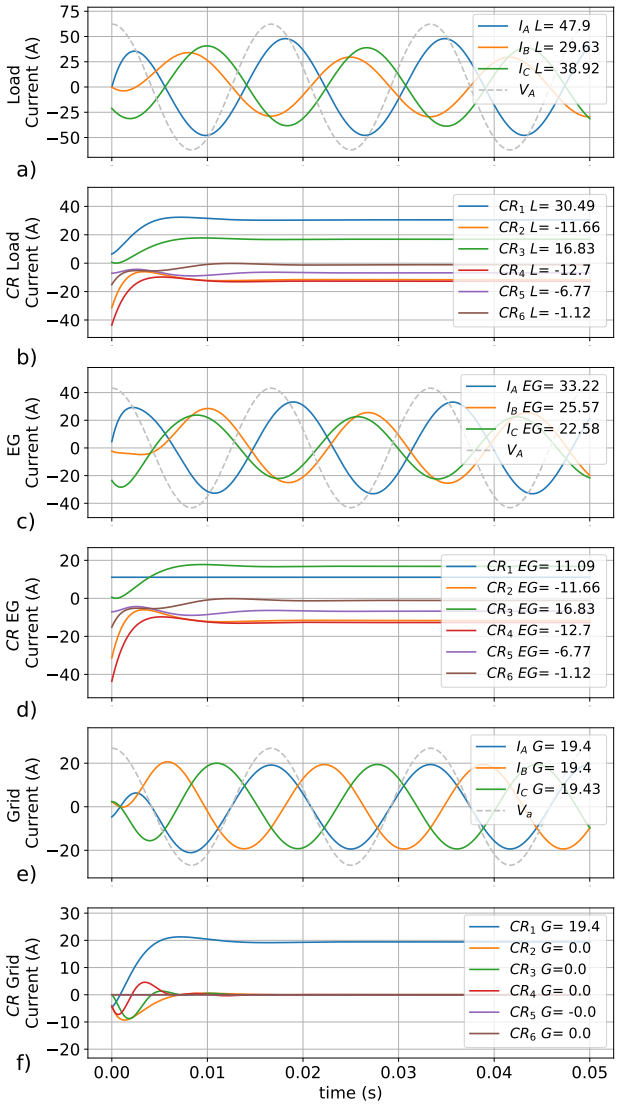

Fig. 4. Current of elements in simulation one. a) current of load in ABC domain, b) Current of load in SoCR domain, c) current supplied for the EG in ABC domain, d) curient of EG in SoCR domain, e) corriente proporcionada por la red en el dominio del tiempo y f) corriente proporcionada por la red en el dominio SoCR

EGs, and 4) an unbalanced load. The grid and the load have current sensors connected to CR meters. The CR meter of the load has the CR_{2-6} components connected to the EG for inefficiencies compensation through the MGCC, and the CR meter is used to monitor the state of the main grid. The EG has connected a constant value for the CR_1 of 11.09, this value is used to simulate the active power available from an energy resource connected to the EG, for example solar or wind energy. The simulation is carried out with an unbalanced load formed by a resistive-inductive element with a resistance of 3Ω and an inductance of $5mH$ in the A phase, a resistive-inductive element with a resistance of 3Ω and an inductance of $13mH$ in the B phase, and a resistive-capacitive element with a capacitance of $1.5mF$ and a resistance of 4Ω in the C phase.

Figure 4 shows the operation of the SoCR of the figure 5. The figure 4 has six graphs of current, three in the ABC domain and three in the SoCR domain related to blocks 1, 2 and 4 of figure 5. Figures 4 a), c) and e) plot the current in the ABC domain of the load, the EG and the main grid,

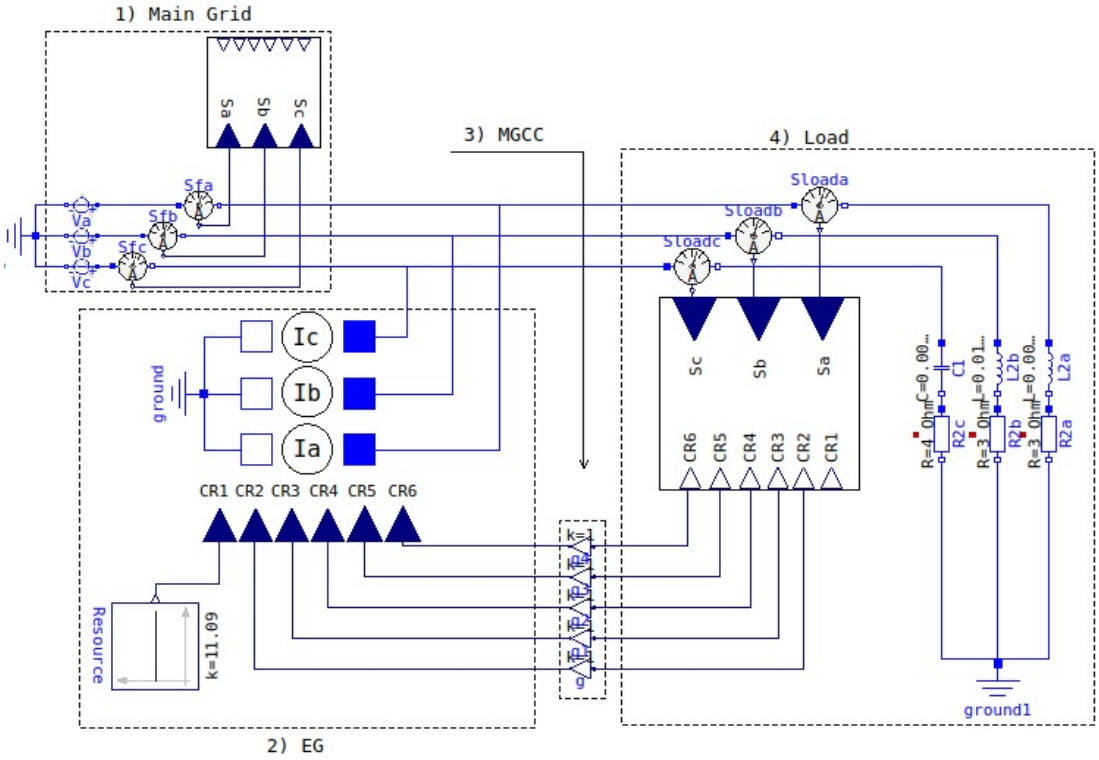

Fig. 5. Simulation one schematic for SoCR validation.

respectively; while the figures 4 b), d) and f) plot the SoCR current of the load, the EG and the grid, respectively. I_A L, I_B L, I_C L and V_A lines represent the phase current A, phase current B, phase current C and grid voltage V_A. The grid voltage V_A is not scaled and is plotted to show the voltage/current phase-lag.

Figures 4 a) and c) show two unbalanced three-phase systems with no obvious correlation: the amplitudes of each phase are different, and the phase-lag of $\frac{2\pi}{3}$ do not correspond, however, the figures 4 b and d show that in steady state the values CR_{2-6} of the EG and the load are equal; the only different value in the SoCR domain between the load and the EG is CR_1 and this is because the EG has an associated energy resource that may be different a load requires.

Figure 4 e) shows that the current delivered by the power grid is three-phase and balanced, in addition, the grid current I_A G is in phase with the voltage V_A; both signals in phase mean that the power grid is supplying only active power and that EG is supplying the inefficiencies by means of the $SoCR$. Figure 4 f) shows that after the transient, the references CR_{2-6} are zero and that the reference CR_1 is stabilized at a constant value of $19.04A$ corresponding to the maximum value of the three-phase current delivered by the main grid, this means that if the current is in phase with the voltage, and the value CR_1 corresponds to the maximum value of current, then the value CR_1 is proportional to the active power supplied or received by the main grid. In conclusion, all the graphs in the figure 4 show that 1) in the ABC domain it is not easy to determine the references for the compensation of inefficiencies, while in the SoCR domain the five CR_{2-6} allow to establish constant values to improve the quality of electricity and 2) the SoCR values are constant after the current transients.

Table I shows a summary of the SoCR values in the figure 4. This table has in the columns the load, the EG and the main grid and in the rows the CR of each one. Table I shows that $ICR_1^{Grid} + ICR_1^{DC/AC} = ICR_1^{load}$, that the CR_{2-6} of the main grid are equal to zero, and that the CR_{2-6} of the load and the EG are equal, fulfilling the equation 23.

TABLE I
CR VALUES OF SIMULATION ONE.

	Load	EG	Grid
ICR_1	30.49	11.09	19.4
$ICR2$	-11.66	-11.66	0
ICR_3	16.83	16.83	0
ICR_4	-12.7	-12.7	0
ICR_5	-6.77	-6.77	0
ICR_6	-1.12	-1.12	0

B. MG simulation with equal inefficiencies distribution among its EG

The figure 6 is divided into four blocks: 1) the main grid, 2) three EGs that receive CR, 3) a MGCC that distributes the inefficiencies proportionally and 4) two unbalanced loads with contactors that turn on at $0.8s$ and $0.16s$ to validate the operation of the MG at load changes.

In this simulation the inefficiencies of the load are distributed among the EGs of the MG by means of a MGCC that distributes the CR_{2-6} of the load among the EGs. On the other hand, the CR_1 values of the EGs have connected constant CR_1 values of $15A$, $9.09A$ and $-6A$ to represent solar and wind generation and battery storage. CR_1 of EG of batteries has negative value to highlight the behavior of the system when it is storing energy.

Figure 7 a) shows the current demanded by the unbalanced load in the ABC domain. I_A L, I_B L, I_C L and V_A are

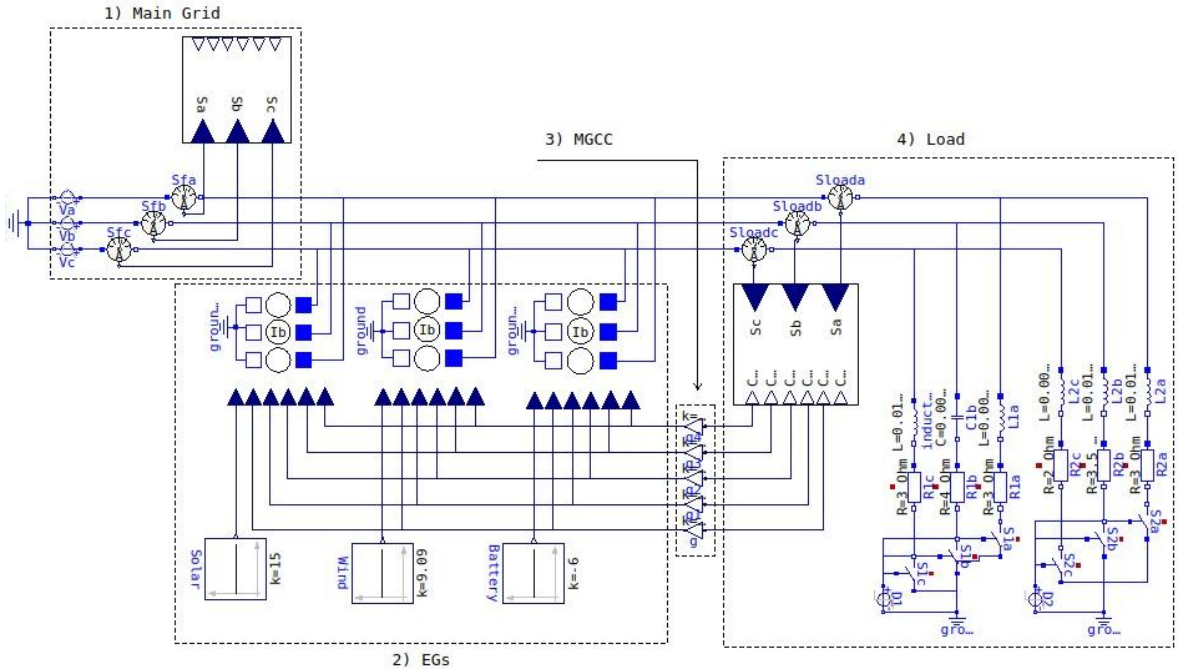

Fig. 6. Simulation two, a MG with three EGs and variable load for validating SoCR in inefficiencies distribution.

the phase current A, phase current B, phase current C and grid voltages V_A, respectively. The V_A is not to scale, but is plotted to highlight the phase-lag between voltage V_A and current I_A. This figure shows the current demanded by the load, which varies in time due to contactors operation in three instants of time: 1) at the beginning of the simulation no contactor has been activated, therefore, the current demanded by the load is zero; 2) at the instant $t = 0.08s$ the contactor of the first unbalanced load is activated; 3) at the instant $t = 0.16s$ the second contactor is activated and the amount of current demanded increases, however, the characteristics of unbalances change. The demand of current at time instant 2 shows that the current of the phase A has peak values larger than the phase B and C, while time instant 3 shows that the phase C has peak larger than the other two phases; In the ABC domain it cannot be concluded if the currents are $\frac{2\pi}{3}$ phase-lag, however, the load currents have different $\frac{2\pi}{3}$ phase-lag because the inductive and capacitive values are not equal; furthermore, there is evidence of a phase-lag between V_A and I_A L. Figure 7 b) shows the current of the load in the SoCR domain; in this figure, the CR of the load shows the three times of figure 7 a) and it is seen that there is a transient at each current change, however, the CR are constant values when the signal is stabilized. In figure 7 b), the SoCR values are zero before the contactor input, due to there is not load, and CR are different at times two and three due to there are inefficient loads.

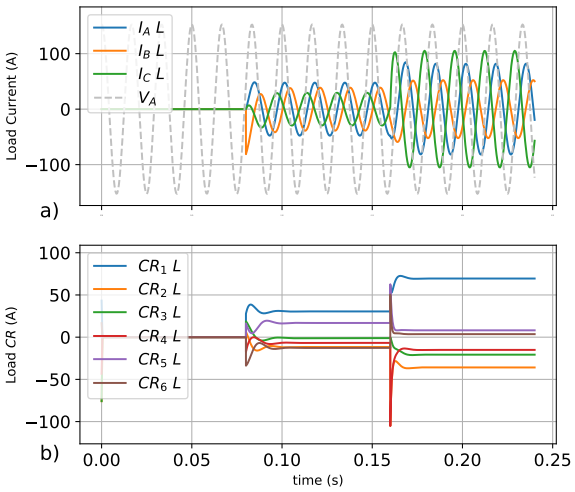

Fig. 7. Current of load, a) in ABC domain b) in SoCR domain.

the figure 8 a) shows the current delivered by the main grid in the ABC domain. Figure 8 a) shows that the signal of currents are three-phase and balanced over the three time instants, meaning that the power grid is delivering or receiving active power. The three time instants are described below: 1) in the first time instant the load does not demand power and the power demanded by the battery is less than the power supplied by the solar and wind resource, therefore, the electric grid receives active power. This phenomenon is shown in figure 8 a), since the V_A is in opposite-phase with the current of phase A. 2) In the second instant of time the electrical main grid is delivering power; in this instant of time V_A and the current of phase A are in phase, this is due to the fact that the power demanded by the load and the power demanded by the battery is greater than the power supplied by the solar and wind resource, therefore, the main grid has to supply active power. 3) in the third instant of time the main grid continues to deliver active power but in greater quantity, this is because the second contactor was activated, then, the load is demanding greater amount of current.

The figure 8 b) graphs the current delivered by the power grid in the SoCR domain. This graph shows that the value CR_1 is the only value different from zero in the three instants of time, in steady state, while the values CR_{2-6} are zero, in

steady state. The figure shows that there are transients at each change of the load current value where the CR values are random. The figure 8 shows that the CR_1 value of the main grid is negative the first instant of time, this means that the main grid is receiving power, while the other two instants of time are positive, i.e. the main grid is supplying power. The figures 8 a) and b) allow us to conclude that inefficiencies can be distributed among the EGs of an RM by means of SoCR, that the SoCR method increases the use of the MG's equipment, improves the quality of the electrical energy and increases stability related to the quality power.

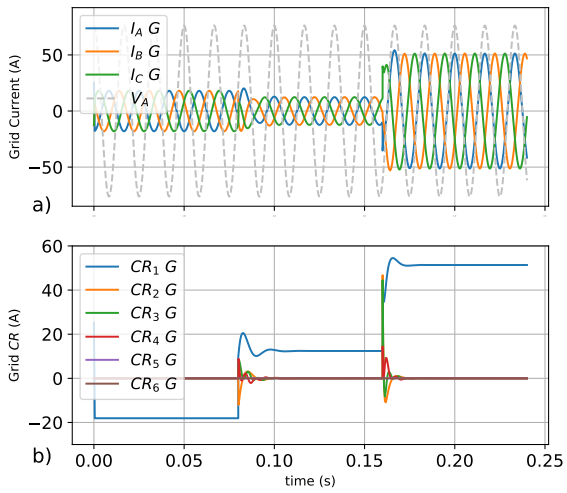

Fig. 8. Current of main grid, a) in ABC domain y b) In SoCR domain.

The figure 9 a), b) and c) shows the current of the EGs connected to solar, wind and batteries, respectively. In the three graphs, I_A, I_B, I_C and V_A are the phase current A, phase current B, phase current C and grid voltage V_A, respectively for each EG. Each graph in the figure 9 has three time instants because the load demands different inefficiencies at each time instant. At the first time instant, figure 9 a) and b) show that the phase current A and voltage A are in phase, and the currents are three-phase balanced, which means that power is being delivered. At this point in time the solar and wind generation EGs provide active power and do not compensate for inefficiencies. On the other hand, the 9 c) shows V_A in opposite-phase with the phase current A, with the three balanced currents, which means receiving power. At this point in time the battery demands active power. At the second instant of time the load starts demanding inefficiencies, however, the inefficiencies are distributed among the three EGs equally. The figure 9 a) and b) provide unbalanced three-phase currents, however, the current provided by the three EGs are not comparable between the three EGs neither in magnitude nor phase-lag, highlighting that establishing references in the ABC domain is not trivial and evidencing that SoCR is a tool that allows the distribution of inefficiencies between the EGs of an MG.

IV. Conclusion

In the content of this document a method to distribute the electrical inefficiencies related to reactive energy and imbalances in an MG is developed; for the development of SoCR method, the concept of three-phase systems as spatial vectors and the representation of imbalances by means of symmetrical components are used, the dq transformation is used and the equations SoCR are developed for the implementation of the proposed method in hardware and simulation.

In this document, two scenarios are simulated to demonstrate how SoCR works. The first scenario is simulated with a current source that receives as input parameters CR, an unbalanced load and the main grid; the second scenario is composed of three EGs that receive CR and have constant values connected in CR_1 to simulate energy resources, a load variable in time by means of contactors and the main grid to represent a MG. The first simulation shows that the SoCR represents in six constant values an unbalanced three-phase system with reactive power demand. In addition, it establishes the current values that an EG must supply to guarantee the quality of the energy. The first simulation shows that the CR are constant values and that in steady state the main grid only provides active power. The second simulation, the MG, shows that the SoCR is used to distribute the inefficiencies among the EGs of MG achieving that the maing grid only provides active power and guaranteeing quality power in the MGs or improving it in case the EGs do not have power availability to supply inefficiencies. The results of the second simulation evidence the functioning of SoCR when the EGs do not have to compensate inefficiencies and when they have to compensate all inefficiencies in a distributed way. In addition, the second scenario shows that determining references of current to compensate for inefficiencies in the ABC domain is not trivial, much less its distribution among EGs, while SoCR allows the distribution of inefficiencies and even facilitates optimization algorithms to determine equipment operating points in MGs. The second simulation shows that the CR works even when there are transients in the load. The results of simulations show that the value CR_1 is related to the active power.

The simulation results lead to the conclusion that SoCR can set a benchmark for distribution of MG inefficiencies among EGs, improve power quality, and enhance energy efficiency. The use of EGs can avoid the purchase of an active power filter to compensate for inefficiencies, and finally, it is shown that SoCR increases the equipment usage factor of an MG, which means reducing costs and decreasing pollutants from equipment manufacturing.

The SoCR for distribution could be implemented in commercial EG, therefore, this proposed method could mean a way to potentialize the energy transition in the MG implementation.

The last conclusion of this document is that this proposal favors the EG use of as sources of current and not as sources of voltage, suggesting that EGs functioning as sources of current can provide stability and quality of electrical energy in a similar way to EGs functioning as a source of voltage, which seeking to imitate the operation of conventional electrical machines. This paper proposes a paradigm shift and the evaluation of this possibility.

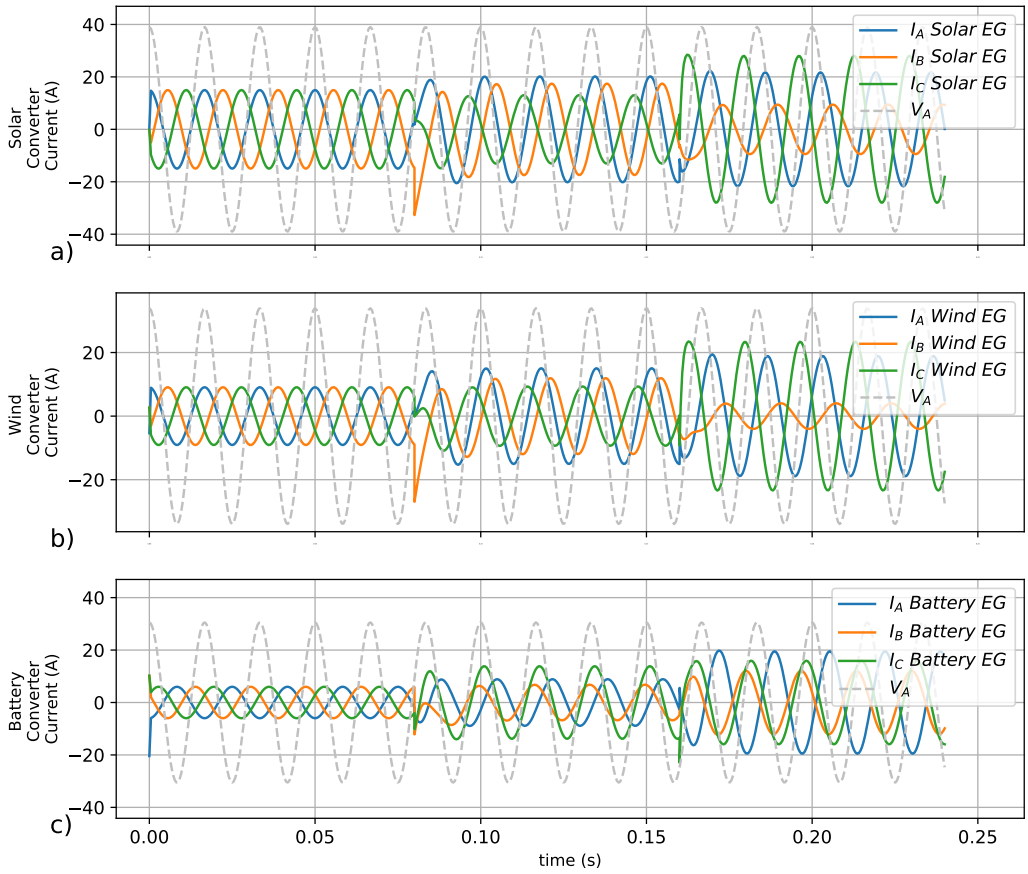

Fig. 9. Current of EGs in ABC domain, a) current of solar resource, b) current of wind resources y c) current of storage system

APPENDIX A
THEORETICAL BACKGROUND: A GEOMETRICAL DEDUCTION OF dq TRANSFORMATION AND SYMMETRICAL COMPONENTS

A three-phase system X can be represented as a space vector. The equation 24 represents a three phase system of amplitude M, angular frequency $w = 2\pi f$ and frequency f.

$$X = \begin{bmatrix} X_a \\ X_b \\ X_c \end{bmatrix} = \begin{bmatrix} M_x \cos(wt) \\ M_x \cos\left(wt - \frac{2\pi}{3}\right) \\ M_x \cos\left(wt - \frac{4\pi}{3}\right) \end{bmatrix} \tag{24}$$

The space vector is obtained as the vectorial sum resulting from the three phases X_A, X_B and X_C at each instant of time. The table contains the data of a three-phase system for any M_x of the equation 24 which is represented in the figure 10. This table is composed of five rows: row 1 the angle of the position of the space vector in degrees, row 2 the time of a cycle of the three-phase system, row three, four and five have the phases X_A, X_B and X_C respectively. The data of the table II is used to construct the figure 10.

The figure 10 a), b), c), d), e) and f) shows the concept of space vector. Each graph in figure 10 is related to each angle phi and time of the table II. Each graph in the figure has three axes shifted by 120 degrees for the phases X_A, X_B and X_C. The phases X_A, X_B and X_C are represented in color blue, orange and green respectively. The vectorial sum of the three phases is represented with a black vector that has amplitude $\frac{3}{2}M_x$ and is oriented in the angle ϕ of the table II. The figure 10 allows to conclude that a three-phase system is a vector that rotates with the angular frequency w and in the direction established by the phase sequences; in this example the direction of rotation is that of the hands of the clock.

TABLE II
DATA TO GRAPH A THREE-PHASE SYSTEM AS SPACE VECTOR .

ϕ	0	60	120	180	240	300	360
t	0	$\frac{1}{6f}$	$\frac{2}{6f}$	$\frac{3}{6f}$	$\frac{4}{6f}$	$\frac{5}{6f}$	$\frac{6}{6f}$
P_A	M_x	$\frac{M_x}{2}$	$-\frac{M_x}{2}$	$-M_x$	$-\frac{M_x}{2}$	$\frac{M_x}{2}$	M_x
P_B	$-\frac{M_x}{2}$	$\frac{M_x}{2}$	M_x	$\frac{M_x}{2}$	$-\frac{M_x}{2}$	$-M_x$	$-\frac{M_x}{2}$
P_C	$-\frac{M_x}{2}$	$-M_x$	$-\frac{M_x}{2}$	$\frac{M_x}{2}$	M_x	$\frac{M_x}{2}$	$-\frac{M_x}{2}$

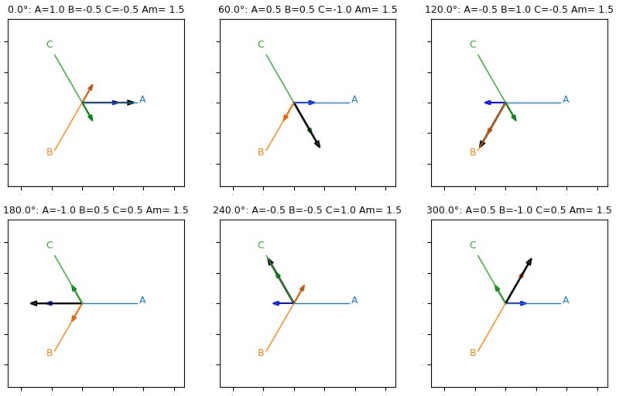

Fig. 10. Three-phase system representation as a spacial vector.

The second part in the understanding of the proposed system is a geometric interpretation of the dq transform. If the three-phase system X of the equation 24 is used as a reference, with any value of M_x, and a second three-phase system Y is proposed, as in the equation 25 with a lag phi and magnitude M_y, both vectors will have the same lag phi as in the figure 11. The rotation of both vectors with the same frequency and the same sequence makes the projection of Y over X constant. Due to this, a space vector X_d of magnitude 1 and with the direction of X and a space vector with X_q magnitude 1 and in quadrature direction of X are used to decompose Y over X. X_d and X_q are represented in the equation 26 and 27 respectively.

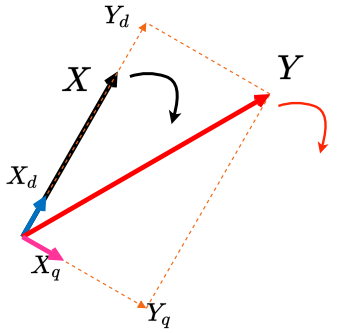

Fig. 11. proyección de un vector espacial sobre eje directo y eje en cuadratura de otro vector espacial en un instante de tiempo.

$$Y = \begin{bmatrix} Y_A \\ Y_B \\ Y_C \end{bmatrix} = \begin{bmatrix} M_y \cos(wt - \phi) \\ M_y \cos\left(wt - \frac{2\pi}{3} - \phi\right) \\ M_y \cos\left(wt - \frac{4\pi}{3} - \phi\right) \end{bmatrix} \tag{25}$$

$$X_d = \begin{bmatrix} X_{d_A} \\ X_{d_B} \\ X_{d_C} \end{bmatrix} = \begin{bmatrix} \cos(wt) \\ \cos\left(wt - \frac{2\pi}{3}\right) \\ \cos\left(wt - \frac{4\pi}{3}\right) \end{bmatrix} \tag{26}$$

$$X_q = \begin{bmatrix} X_{q_A} \\ X_{q_B} \\ X_{q_C} \end{bmatrix} = \begin{bmatrix} -\sin(wt) \\ -\sin\left(wt - \frac{2\pi}{3}\right) \\ -\sin\left(wt - \frac{4\pi}{3}\right) \end{bmatrix} \tag{27}$$

the figure 11 represents two three-phase systems as spatial vectors, however, if X is voltage and Y is current, then the projection of Y over X, Y_d, is related to active power and the projection of Y over a quadrature component of X, Y_q, is related to reactive power. The projections Y_d and Y_q can be calculated as $Y_d = Y \cdot X_d$ and $Y_q = Y \cdot X_q$. These operations can be written as the equation 28 where the $\frac{2}{3}$ is used to reduce the amplification presented in the figure 10.

$$\begin{bmatrix} Y_d \\ Y_q \end{bmatrix} = \frac{2}{3} * \begin{bmatrix} \cos(\omega t) & \cos\left(\omega t - \frac{2\pi}{3}\right) & \cos\left(\omega t - \frac{4\pi}{3}\right) \\ -\sin(\omega t) & -\sin\left(\omega t - \frac{2\pi}{3}\right) & -\sin\left(\omega t - \frac{4\pi}{3}\right) \end{bmatrix} \begin{bmatrix} Y_A \\ Y_B \\ Y_C \end{bmatrix} \tag{28}$$

The equation 29 presents dq transformation in a general way based on the equation 28. In the equation 28 the coefficient is changed from $\frac{2}{3}$ to $\sqrt{2/3}$, this due to in the equation 29 the transposed one is equal to the inverse, therefore, it is used when the process requires to return to its original condition.

$$T^1_{ABC \to dq} = \sqrt{\frac{2}{3}} \begin{bmatrix} \cos(\omega t) & \cos\left(\omega t - \frac{2\pi}{3}\right) & \cos\left(\omega t - \frac{4\pi}{3}\right) \\ -\sin(\omega t) & -\sin\left(\omega t - \frac{2\pi}{3}\right) & -\sin\left(\omega t - \frac{4\pi}{3}\right) \end{bmatrix} \tag{29}$$

The equation 29 is used for a three-phase system of positive sequence , however, if there is three-phase system in a negative sequence, dq transformation can be written as in the equation 30.

$$T^2_{ABC \to dq} = \sqrt{\frac{2}{3}} \begin{bmatrix} \cos(\omega t) & \cos\left(\omega t + \frac{2\pi}{3}\right) & \cos\left(\omega t + \frac{4\pi}{3}\right) \\ -\sin(\omega t) & -\sin\left(\omega t + \frac{2\pi}{3}\right) & -\sin\left(\omega t + \frac{4\pi}{3}\right) \end{bmatrix} \tag{30}$$

las ecuaciones 31 y 32 son las inversas de las ecuaciones 29 y 30 y son presentadas en este documento para orientar al lector.

$$T^2_{ABC \to dq}{}^{-1} = \sqrt{\frac{2}{3}} \begin{bmatrix} \cos(\omega t) & -\sin(\omega t) \\ \cos\left(\omega t - \frac{2\pi}{3}\right) & -\sin\left(\omega t - \frac{2\pi}{3}\right) \\ \cos\left(\omega t - \frac{4\pi}{3}\right) & -\sin\left(\omega t - \frac{4\pi}{3}\right) \end{bmatrix} \tag{31}$$

$$T^2_{ABC \to dq}{}^{-1} = \sqrt{\frac{2}{3}} \begin{bmatrix} \cos(\omega t) & -\sin(\omega t) \\ \cos\left(\omega t + \frac{2\pi}{3}\right) & -\sin\left(\omega t + \frac{2\pi}{3}\right) \\ \cos\left(\omega t + \frac{4\pi}{3}\right) & -\sin\left(\omega t + \frac{4\pi}{3}\right) \end{bmatrix} \tag{32}$$

dq transformation is used in electrical engineering applications as electrical machines and in power electronics application related to active and reactive power, harmonics, unbalances, serial and parallel compensation, among others.

The last step to understand CR is the symmetric components method. The decomposition into symmetric components states that an unbalanced three-phase system of current I can be decomposed as $I = I_0 + I_1 + I_2$, where I_0 is the zero sequence, I_1 is the positive sequence and I_2 is the negative sequence. The figure 12 shows the decomposition of a balanced three-phase system into its symmetric components. Figure 12 a) shows the phasors of an unbalanced

three-phase system, figure 12 b) shows the zero sequence of an unbalanced three-phase system, figure 12 c) shows the positive sequence of an unbalanced three-phase system and figure 12 d) shows the negative sequence of three-phase system. The decomposition of the figure 12 can be done with the equation 33, where the vectors on the right side of the equality correspond to the three-phase systems of zero sequence, positive sequence and negative sequence respectively.

$$\begin{bmatrix} I_a \\ I_b \\ I_c \end{bmatrix} = \begin{bmatrix} I_{0_A} \\ I_{0_b} \\ I_{0C} \end{bmatrix} + \begin{bmatrix} I_{1_A} \\ I_{1_B} \\ I_{1_C} \end{bmatrix} + \begin{bmatrix} I_{2_A} \\ I_{2_B} \\ I_{2_C} \end{bmatrix} \quad (33)$$

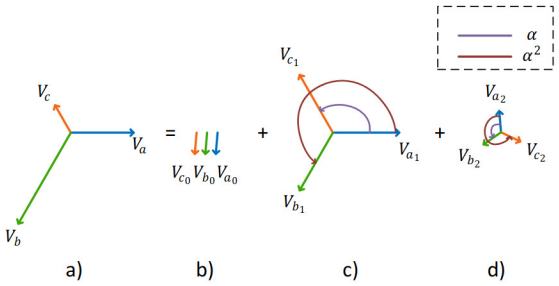

Fig. 12. Cambiar V por I para que corresponda con el texto. Descomposición de sistema desbalanceado en componentes simétricas. a) sistema desbalanceado; b) sistema de secuencia cero; c) sistema de secuencia positiva ; y d) sistema de secuencia negaiva.

ACKNOWLEDGMENT

The authors would like to thank...

Author thanks ... ." Sponsor and financial support acknowledgments

REFERENCES

[1] S. Rathor and D. Saxena, "Energy management system for smart grid: An overview and key issues," *International Journal of Energy Research*, vol. 44, no. 6, pp. 4067–4109, 2020.

[2] W. Liu, X. Zhang, and S. Feng, "Does renewable energy policy work? evidence from a panel data analysis," *Renewable Energy*, vol. 135, pp. 635 – 642, 2019. [Online]. Available: http://www.sciencedirect.com/science/article/pii/S096014811831468X

[3] F. Nicolli and F. Vona, "Energy market liberalization and renewable energy policies in oecd countries," *Energy Policy*, vol. 128, pp. 853 – 867, 2019. [Online]. Available: http://www.sciencedirect.com/science/article/pii/S0301421519300187

[4] M. Aguirre and G. Ibikunle, "Determinants of renewable energy growth: A global sample analysis," *Energy Policy*, vol. 69, pp. 374 – 384, 2014. [Online]. Available: http://www.sciencedirect.com/science/article/pii/S0301421514001451

[5] M. Jirdehi, V. Tabar, S. Ghassemzadeh, and S. Tohidi, "Different aspects of microgrid management: A comprehensive review," *Journal of Energy Storage*, vol. 30, 2020.

[6] I. Serban, S. Cespedes, C. Marinescu, C. Azurdia-Meza, J. Gomez, and D. Hueichapan, "Communication requirements in microgrids: A practical survey," *IEEE Access*, vol. 8, pp. 47 694–47 712, 2020.

[7] L. Hernández-Callejo, "A comprehensive review of operation and control, maintenance and lifespan management, grid planning and design, and metering in smart grids," *Energies*, vol. 12, no. 9, 2019.

[8] F. Nejabatkhah, Y. W. Li, and H. Tian, "Power quality control of smart hybrid ac/dc microgrids: An overview," *IEEE Access*, vol. 7, pp. 52 295–52 318, 2019.

[9] J. Schiffer, D. Zonetti, R. Ortega, A. M. Stanković, T. Sezi, and J. Raisch, "A survey on modeling of microgrids—from fundamental physics to phasors and voltage sources," *Automatica*, vol. 74, pp. 135 – 150, 2016. [Online]. Available: http://www.sciencedirect.com/science/article/pii/S0005109816303041

[10] S. Muhanji, A. Muzhikyan, and A. Farid, "Distributed control for distributed energy resources: Long-term challenges and lessons learned," *IEEE Access*, vol. 6, pp. 32 737–32 753, 2018.

[11] A. Vijay, S. Doolla, and M. Chandorkar, "Unbalance mitigation strategies in microgrids," *IET Power Electronics*, vol. 13, no. 9, pp. 1687–1710, 2020.

[12] I. Vechiu, O. Curea, and H. Camblong, "Transient operation of a four-leg inverter for autonomous applications with unbalanced load," *IEEE Transactions on Power Electronics*, vol. 25, no. 2, pp. 399–407, 2010.

[13] Y. Yang, F. Blaabjerg, H. Wang, and M. Simões, "Power control flexibilities for grid-connected multi-functional photovoltaic inverters," *IET Renewable Power Generation*, vol. 10, no. 4, pp. 504–513, 2016.

[14] S. Mousazadeh Mousavi, A. Jalilian, M. Savaghebi, and J. Guerrero, "Power quality enhancement and power management of a multifunctional interfacing inverter for pv and battery energy storage system," *International Transactions on Electrical Energy Systems*, vol. 28, no. 12, 2018, cited By 6.

[15] M. M. Amin and O. A. Mohammed, "Development of high-performance grid-connected wind energy conversion system for optimum utilization of variable speed wind turbines," *IEEE Transactions on Sustainable Energy*, vol. 2, no. 3, pp. 235–245, 2011.

[16] L. Wang, C. Lam, and M. Wong, "Multifunctional hybrid structure of svc and capacitive grid-connected inverter (svc//cgci) for active power injection and nonactive power compensation," *IEEE Transactions on Industrial Electronics*, vol. 66, no. 3, pp. 1660–1670, 2019.

[17] D. C. Silva Júnior, J. G. Oliveira, P. M. de Almeida, and C. Boström, "Control of a multi-functional inverter in an ac microgrid – real-time simulation with control hardware in the loop," *Electric Power Systems Research*, vol. 172, pp. 201 – 212, 2019. [Online]. Available: http://www.sciencedirect.com/science/article/pii/S0378779619301099

[18] T. Caldognetto, P. Tenti, P. Mattavelli, S. Buso, and D. I. Brandao, "Cooperative compensation of unwanted current terms in low-voltage microgrids by distributed power-based control," in *2015 IEEE 13th Brazilian Power Electronics Conference and 1st Southern Power Electronics Conference (COBEP/SPEC)*, 2015, pp. 1–7.

[19] S. Hoseinnia, M. Akhbari, M. Hamzeh, and J. Guerrero, "A control scheme for voltage unbalance compensation in an islanded microgrid," *Electric Power Systems Research*, vol. 177, p. 106016, 2019. [Online]. Available: http://www.sciencedirect.com/science/article/pii/S0378779619303359

[20] M. R. Iravani and M. Karimi-Ghartemani, "Online estimation of steady state and instantaneous symmetrical components," *IEE Proceedings - Generation, Transmission and Distribution*, vol. 150, no. 5, pp. 616–622, Sep. 2003.

First A. Author (M'76-SM'81-F'87) Biography text here. The authors may choose to include biographies at the end of regular papers. Biographies are often not included in conference-related papers. This author became a Member (M) of IAENG in 1976, a Senior Member (SM) in 1981, and a Fellow (F) in 1987. The first paragraph may contain a place and/or date of birth (list place, then date). Next, the author's educational background is listed. The degrees should be listed with type of degree in what field, which institution, city, state, and country, and year degree was earned. The author's major field of study should be lower-cased.

The second paragraph uses the pronoun of the person (he or she) and not the author's last name. It lists military and work experience, including summer and fellowship jobs. Job titles are capitalized. The current job must have a location; previous positions may be listed without one. Information concerning previous publications may be included. Try not to list more than three books or published articles. The format for listing publishers of a book within the biography is: title of book (city, state: publisher name, year) similar to a reference. Current and previous research interests end the paragraph.

The third paragraph begins with the author's title and last name (e.g., Dr. Smith, Prof. Jones, Mr. Kajor, Ms. Hunter). List any memberships in professional societies other than the IAENG. Finally, list any awards and work for IAENG committees and publications. If a photograph is provided, the biography will be indented around it. The photograph is placed at the top left of the biography. Personal hobbies will be deleted from the biography.